Journal of Theoretical Biology
April 2021, Volume 515, Pages 110597 (12p.)
https://doi.org/10.1016/j.jtbi.2021.110597
https://archimer.ifremer.fr/doc/00676/78768/

The promise of dawn: microalgae photoacclimation as an optimal control problem of resource allocation

Mairet Francis [1], Bayen Térence [2]

[1] Ifremer, Physiology and Biotechnology of Algae laboratory, rue de l'Ile d'Yeu, 44311 Nantes, France
[2] Avignon Université, Laboratoire de Mathématiques d'Avignon (EA 2151) F-84018, France

Addresses mail : francis.mairet@ifremer.fr ; terence.bayen@univ-avignon.fr

Abstract :

Photosynthetic microorganisms are known to adjust their photosynthetic capacity according to light intensity. This so-called photoacclimation process is thought to maximize growth at equilibrium, but its dynamics under varying conditions remains less understood. To tackle this problem, microalgae growth and photoacclimation are represented by a (coarse-grained) resource allocation model. Using optimal control theory (the Pontryagin maximum principle) and numerical simulations, we determine the optimal strategy of resource allocation to maximize microalgal growth rate over a time horizon. We show that, after a transient, the optimal trajectory approaches the optimal steady state, a behavior known as the turnpike property. Then, a bi-level optimization problem is solved numerically to estimate model parameters from experimental data. The fitted trajectory represents well a Dunaliella tertiolecta culture facing a light down-shift. Finally, we study photoacclimation dynamics under day/night cycle. In the optimal trajectory, the synthesis of the photosynthetic apparatus surprisingly starts a few hours before dawn. This anticipatory behavior has actually been observed both in the laboratory and in the field. This shows the algal predictive capacity and the interest of our method which predicts this phenomenon.

Graphical abstract

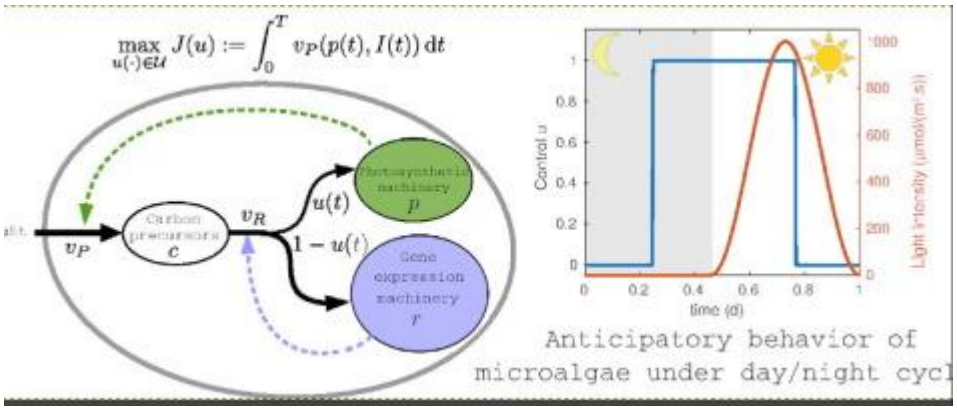

Highlights

► Facing a light shift, the optimal strategy of photoacclimation is a *turnpike*. ► A bi-level optimization problem is solved to estimate model parameters. ► Under day/night cycle, the model predicts that microalgae anticipates the dawn. ► The algal anticipatory strategy is in line with laboratory and field observations.

Keywords : Turnpike, Bi-level optimization, Microalgal growth model, Photosynthetic apparatus, Anticipatory behavior

1. Introduction

Microalgae are key players in the ocean (Falkowski and Raven, 2007), and they also represent a promising resource for various markets (feed, health, etc) (Spolaore et al., 2006). These microorganisms adjust their photosynthetic apparatus according to the light they received: *e.g.*, if light is in excess, the photosynthetic apparatus will decrease (MacIntyre et al., 2002). This so-called photoacclimation process is an important factor to consider when estimating net primary production in the ocean from satellite chlorophyll measurements (Graff et al., 2016), or when optimizing microalgal production given the interplay between self-shading and light limitation (Bernard et al., 2015; De Mooij et al., 2017).

Mathematical models have been proposed to understand and predict microalgal photoacclimation. They can be divided into two types: empirical models, mainly based on experimental observations (*e.g.*, Geider et al. (1998); García-Camacho et al. (2012); Bernard et al. (2015); Nikolaou et al. (2016); Straka and Rittmann (2018)), and optimality-based models. The latter type relies on the hypothesis, widespread for predictive models in biology, that evolution has resulted in organisms having optimal performances (Sutherland, 2005). Microbial growth can thus be formalized as an optimization problem, where resources should be allocated between different sectors in order to maximize the growth rate for exemple. In this framework, photoacclimation models based on static optimization have been proposed by Shuter (1979); Armstrong (2006); Geider et al. (2009); Jahn et al. (2018); Faizi and Steuer (2019); Zavřel et al. (2019). These models correctly represent photoacclimation in a constant environment. Nonetheless, light supply is always changing, because of the sunpath, the presence of clouds, the position of the cell in the water column, etc. In this context, Talmy et al. (2013) have determined a fixed resource allocation which maximizes the growth over a time window under light fluctuations. However, this study still neglects photoacclimation dynamics. Instantaneous optimization has been proposed to represent photoacclimation under variable conditions (Wirtz and Pahlow, 2010). That is, at each instant, the chlorophyll content is adjusted so as to maximize instantaneous growth. It appears that such a strategy is not necessarily optimal over the long term. Generally, one can determine a strategy to maximize growth over a time window. This can be formalized as an optimal control problem, as proposed for example to represent bacterial growth (Pavlov and Ehrenberg, 2013; Waldherr et al., 2015; Giordano et al., 2016). Concerning

photosynthetic microorganisms, to the best of our knowledge, resource allocation optimization over a time window has been tackled only by Cohen and Parnas (1976) and Reimers et al. (2017), focusing on carbon storage over a day-night cycle (and not photoacclimation).

Here a coarse-grained model is proposed to represent microalgae growth and photoacclimation as a resource allocation problem. We first determine the optimal allocation strategy in static conditions, resulting in the classic photoacclimation relationship: the more the light increases, the more the photosynthetic apparatus decreases. Then, we determine the optimal allocation strategy under dynamic conditions, when microalgae face a light shift. Using optimal control theory (Pontryagin' Principle) and numerical simulations (direct methods), we show that the optimal trajectory corresponds to a turnpike, *i.e.*, to quickly adjust the allocation close to the optimal steady state. Then, following our preliminary work (Mairet and Bayen, 2020), a parameter estimation approach - leading to a bi-level optimization problem - is proposed and carried out. This method results in a first proof of concept of how to calibrate dynamic resource allocation model. Finally, optimal allocation strategy under day/night cycles is determined numerically. The simulations reveal that the synthesis of the photosynthetic apparatus begins a few hours before dawn. This behavior is actually observed in several laboratory and field studies (Zinser et al., 2009; John et al., 2012; Hernández Limón et al., 2020), revealing the algal anticipation capacity.

2. Model development

A coarse-grained model of microalgae growth and photoacclimation is proposed, inspired by the works of Shuter (1979) and Giordano et al. (2016).

2.1. Biochemical reactions

The model is based on two macro-reactions, represented in Figure 1. First, CO_2 is fixed to produce small carbon precursors C (in g):

$$CO_2 \xrightarrow{v_P} C,$$

where v_P corresponds to the photosynthetic rate (in g/(g biomass·d)).

The second reaction corresponds to the synthesis of macromolecules, divided into two sectors: the photosynthetic apparatus, including the photosystems and Calvin cycle enzymes P (in g) and the gene expression machinery

(mainly the ribosomes) R (in g):

$$\mathrm{C} \xrightarrow{v_R} u\mathrm{P} + (1-u)\mathrm{R},$$

where v_R (in g/(g biomass·d)) corresponds to the rates of macromolecule synthesis, and $u \in [0,1]$ is the allocation variable representing the part of the flux going to the synthesis of the photosynthetic apparatus. Considering biomass $B = C + P + R$, a mass balance gives the following dynamics:

$$\left|\begin{array}{rcl} \frac{dC}{dt} &=& v_P B - v_R B, \\ \frac{dP}{dt} &=& u v_R B, \\ \frac{dR}{dt} &=& (1-u) v_R B, \\ \frac{dB}{dt} &=& v_P B. \end{array}\right.$$

Now denoting in lowercase the mass fractions (in g/g biomass), *i.e.*, $c = C/B$, $p = P/B$, and $r = R/B$, we finally get

$$\left|\begin{array}{rcccl} \frac{dc}{dt} &=& \frac{1}{B}\frac{dC}{dt} - \frac{C}{B^2}\frac{dB}{dt} &=& v_P(1-c) - v_R, \\ \frac{dp}{dt} &=& \frac{1}{B}\frac{dP}{dt} - \frac{P}{B^2}\frac{dB}{dt} &=& u v_R - p v_P, \\ \frac{dr}{dt} &=& \frac{1}{B}\frac{dR}{dt} - \frac{R}{B^2}\frac{dB}{dt} &=& (1-u) v_R - r v_P. \end{array}\right.$$

2.2. Reaction rates

For the kinetics, we consider that the photosynthetic rate is a function of the photosynthetic apparatus mass fraction and of the light intensity I, i.e., $v_P(p, I)$, with the following assumption

Hypothesis 1. *The function $v_P : [0,1] \times \mathbb{R}_+ \to \mathbb{R}_+$ is of class C^2 and satisfies*

- *For every $p \in [0,1]$, $v_P(p,0) = 0$;*
- *For every $I > 0$, $v_P(0,I) = 0$;*
- *For every $I > 0$, the mapping $v_P(\cdot, I)$ is strictly concave increasing over the interval $[0,1]$.*

Typically, Michaelis-Menten's function

$$v_P(p,I) = k_P \frac{pI}{K + pI}, \tag{1}$$

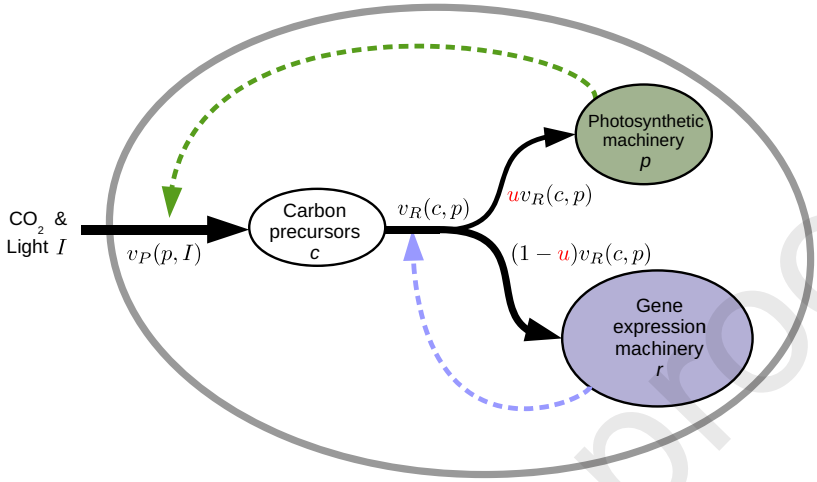

Figure 1: Scheme of the coarse-grained model to represent photoacclimation in microalgae. We assume that microalgae maximize their growth rate by adjusting the resources allocated to the photosynthetic apparatus (through the allocation variable $u \in [0,1]$).

satisfies Hypothesis 1. In this expression, the photosynthetic rate is a function of the product pI, which corresponds to the energy absorbed by the cells. This is in line with mechanistic models of photoacclimation, where the rate depends on the product of the chlorophyll content times the light intensity (see *e.g.*, Geider et al. (1998)).

The rate of macromolecule synthesis depends on the mass fractions of carbon precursors and the gene expression machinery. For sake of simplicity, a mass action kinetics is considered:

$$v_R(c,r) = k_R c r.$$

Note that some numerical simulations with other expressions for both kinetic rates are presented in Appendix A to extend the results presented in the main article.

2.3. Problem statement

Given that $c+p+r=1$, one variable can be removed and we finally get:

$$\left| \begin{array}{rcl} \frac{dc}{dt} & = & v_P(p,I)(1-c) - k_R c(1-c-p), \\ \frac{dp}{dt} & = & uk_R c(1-c-p) - pv_P(p,I). \end{array} \right. \tag{2}$$

Before formalizing the resource allocation problem, we show that the system (2) satisfies the following invariance property. Let us then introduce the set

$$\Omega := \{(c,p) \in (0,1) \times (0,1)\ ;\ c+p \leq 1\}.$$

Lemma 1. *The set Ω is invariant by* (2).

Proof. Whenever $c = 0$ (resp. $p = 0$), it is easily seen that $\dot{c} = v_P(p, I) > 0$ (resp. $\dot{p} = u(t)k_R c(1-c) > 0$), so the positive orthant is invariant. In addition, one has $\dot{c} + \dot{p} = 0$ along $c + p = 1$ so that the line segment $L := \{(c, 1-c)\ ; c \in [0,1]\}$ is also invariant. This ends the proof. □

Since trajectories of (2) starting in L remain in L, we suppose next that initial conditions belong to the (open) invariant domain:

$$\mathcal{D} := \{(c,p) \in (0,1) \times (0,1)\ ;\ c+p < 1\}.$$

We assume that microalgae have acquired through evolution optimal strategy, *i.e.*, they regulate their allocation of resources in order to maximize their growth. To represent this behavior, we are interested in maximizing the photosynthetic rate v_P w.r.t. the allocation of macromolecules synthesis u (corresponding to our control) over a given time period. Thus, we consider the admissible control set defined as:

$$\mathcal{U} = \{u : [0,T] \to [0,1]\ ;\ u \text{ meas}^1.\},$$

in which $T > 0$ is our given time period. The optimization problem under consideration can be then gathered into:

$$\max_{u(\cdot)\in\mathcal{U}} J(u) := \int_0^T v_P(p(t), I)\,\mathrm{d}t, \tag{P}$$

where $(c(\cdot), p(\cdot))$ is the unique solution of (2) starting at a given point $(c_0, p_0) \in \mathcal{D}$ for a given control $u \in \mathcal{U}$.

[1]The abreviation "meas." means measurable in the Lebesgue sense (see Rudin (1987)). Such a class of control functions is very natural in optimal control theory because it allows discontinuous entries which can be optimal in various situations (*e.g.*, bang-bang controls with a finite or an infinite number of discontinuities such as Fuller's phenomenon, see Zelikin and Borisov (1994))

3. Optimal allocation at equilibrium

Our first objective is to determine the optimal allocation at equilibrium, for a constant light intensity $I > 0$. This corresponds to the static optimization problem:

$$\max_{u\in[0,1]} \bar{J}(u) := v_P(p_u, I), \tag{3}$$

where (c_u, p_u) is a steady state of (2) associated with the constant control u and a constant light I, i.e.,

$$\begin{aligned} 0 &= v_P(p_u, I)(1 - c_u) - k_R c_u(1 - c_u - p_u), \\ 0 &= u k_R c_u(1 - c_u - p_u) - v_P(p_u, I)p_u. \end{aligned} \tag{4}$$

Lemma 2. *There is a unique solution $u^* \in [0, 1]$ to (3)-(4) satisfying*

$$v_P((u^*)^2, I) = k_R(1 - u^*)^2.$$

In addition, the corresponding steady-state (c^*, p^*) of (2) is given by

$$\begin{aligned} c^* &= 1 - u^*, \\ p^* &= (u^*)^2. \end{aligned} \tag{5}$$

Proof. Let us first show that $u = 0$ and $u = 1$ are not optimal solutions of (3)-(4). If $u = 0$, then either $v_P(p_u, I) = 0$ or $p_u = 0$ implying in both cases that the objective function $\bar{J}(u)$ is zero. If now $u = 1$, we obtain $v_P(p_u, I)(1 - c_u - p_u) = 0$ and either $p_u = 0$ or $1 - c_u - p_u = 0$. As previously, we can exclude the case $p_u = 0$. But, if now $1 - c_u - p_u = 0$ (with $p_u \neq 0$), we obtain $v_P(p_u, I)(1 - c_u) = 0$, thus $1 - c_u = 0$ and from (4), we get $p_u = 0$ which is not possible. Hence, $u = 1$ is also not optimal.

Let us go back to Problem (3)-(4). From (4), we obtain that any admissible solution of (4) satisfies $p_u = u(1 - c_u)$. Replacing c_u by its value into the first equation then gives

$$g(p, u) := v_P(p, I) - k_R \left(1 - \frac{p}{u}\right)(1 - u) = 0.$$

Problem (3)-(4) then amounts to maximize $u \mapsto \bar{J}(u)$ over $[0, 1]$. Doing so, we apply the classical Karush-Kuhn-Tucker conditions (KKT). Because $u = 0$ and $u = 1$ are not optimal, we can remove the nonbinding constraint $u \in [0, 1]$ and take into account one equality constraint $g(p, u) = 0$. Let then

$\mathcal{L} := \bar{J} + \lambda g$ the Lagrangian associated with (3)-(4). Let u be a maximum of (3)-(4). Then, the stationarity condition

$$\frac{\partial \mathcal{L}}{\partial u} = 0,$$

gives $p = u^2$, and from the equality constraint $g(p, u) = 0$, we obtain

$$v_P(u^2, I) = k_R(1 - u)^2.$$

Since v_P is increasing with $v_P(0, I) = 0$, this equation has a unique solution in $(0, 1)$. The value of (c^*, p^*) follows. □

Using for v_P the Michaelis-Menten function given in (1), u^* is the unique solution in $[0, 1]$ of a polynomial equation of degree four:

$$-Ik_Ru^4 + 2Ik_Ru^3 + (Ik_P - k_RK - Ik_R - k_RK)u^2 + 2k_RKu - k_RK = 0.$$

We can compute this solution as a function of the light intensity. We obtain that the optimal photosynthetic machinery sector at equilibrium p^* is a decreasing function of light intensity I, in line with experimental data of steady-state photoacclimation (MacIntyre et al., 2002), see Fig. 2. Actually, this pattern has already been predicted by steady-state optimization with similar models (*e.g.*, in Armstrong (2006)).

The optimal steady-state enjoys the following stability property (of interest whenever perturbations affect the system).

Proposition 1. *The steady-state (c^*, p^*) of (2) associated with the (constant) control $u = u^*$ is locally stable with two negative eigenvalues.*

Proof. At a steady-state (c, p) of (2) associated with a constant control u, the Jacobian matrix is

$$\begin{bmatrix} -v_P(p, I) - k_R(1 - 2c - p) & \frac{\partial v_P}{\partial p}(p, I)(1 - c) + k_Rc \\ k_Ru(1 - 2c - p) & -k_Ruc - \frac{\partial v_P}{\partial p}(p, I)p - v_P(p, I) \end{bmatrix},$$

and, replacing (c, p, u) by the optimal triplet (c^*, p^*, u^*), it becomes

$$\begin{bmatrix} 0 & \frac{\partial v_P}{\partial p}(p^*, I)u^* + k_R(1 - u^*) \\ -k_Ru^*(u^* - 1)^2 & -k_R(1 - u^*) - (u^*)^2\frac{\partial v_P}{\partial p}(p^*, I) \end{bmatrix}.$$

Since $u^* \in (0, 1)$ and $\frac{\partial v_P}{\partial p} > 0$, the trace and determinant of this matrix are respectively negative and positive which shows that it has exactly two negative eigenvalues. This ends the proof. □

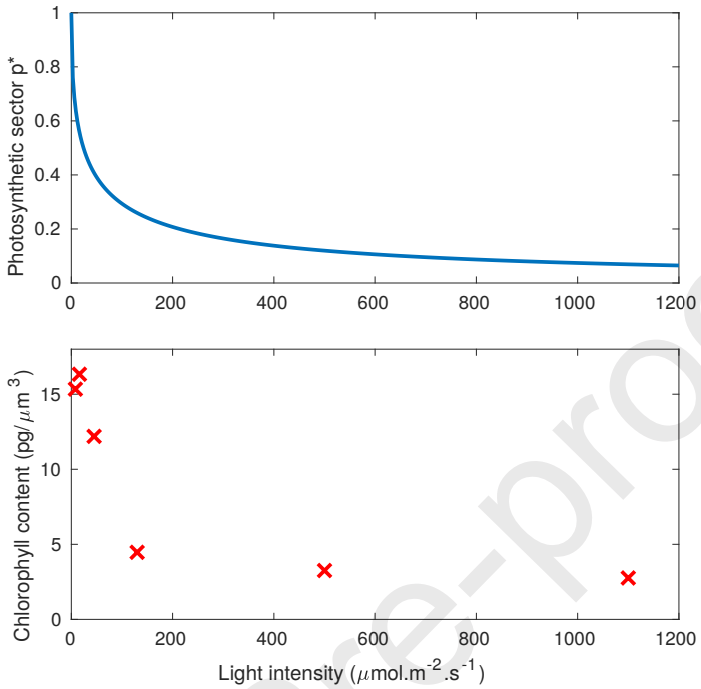

Figure 2: Optimal steady-state allocation for the photosynthetic sector $p^\star$ as a function of light intensity (top), see Lemma 2. This pattern corresponds to the photoacclimation phenomena (MacIntyre et al., 2002), as shown for example by the chlorophyll content measured experimentally for *Dunaliella tertiolecta* (Havelková-Doušová et al., 2004) (bottom).

4. Optimal allocation during a light shift

Our coarse-grained model is now used to study the dynamics of photoacclimation. As a case study, we consider that light intensity is shifted at $t = 0$, and then it remains constant. Our objective is to determine how microalgae can adjust their allocation in order to maximize their growth during the light shift transient. Formally, we thus consider the optimal control problem (P). In the following, $v_P(p, I)$ will be denoted as $v_P(p)$ for sake of simplicity, and v_P' corresponds to its derivative with respect to p.

4.1. Application of the Pontryagin Maximum Principle

Optimal controls are derived using the Pontryagin Maximum Principle (see Pontryagin et al. (1964)). Note that the existence of an optimal control is straightforward (due to the linearity of (2) w.r.t. the control), this follows

from Fillipov's Theorem (Cesari, 1983). Let us now apply Pontryagin's Principle. Doing so, let $H = H(c, p, \lambda_c, \lambda_p, \lambda^0, u)$ be the Hamiltonian associated with (P) (written as a minimum):

$$H := k_R c(1-c-p)\left[u\lambda_p - \lambda_c\right] + v_P(p)\left[\lambda_c(1-c) - \lambda_p p - \lambda^0\right].$$

If u is an optimal control and $x(\cdot) = (c(\cdot), p(\cdot))$ the associated trajectory, there exists $\lambda^0 \leq 0$ and an absolutely continuous map $\lambda = (\lambda_c, \lambda_p) : [0, T] \to \mathbb{R}^2$ such that $(\lambda, \lambda^0) \neq 0$ and satisfying the adjoint equation $\dot{\lambda} = -\frac{\partial H}{\partial x}$, that is:

$$\left|\begin{array}{ll} \dot{\lambda}_c &= -k_R(1-2c-p)(u\lambda_p - \lambda_c) + v_P(p)\lambda_c, \\ \dot{\lambda}_p &= k_R c(u\lambda_p - \lambda_c) + \lambda_p v_P(p) - v_P'(p)\left[\lambda_c(1-c) - \lambda_p p - \lambda^0\right]. \end{array}\right. \tag{6}$$

In addition, since the state is free at the terminal time, transversality conditions imply

$$\lambda_c(T) = \lambda_p(T) = 0. \tag{7}$$

It follows that $\lambda^0 < 0$. Indeed, if $\lambda^0 = 0$, the solution of (6) satisfying the transversality condition would satisfy $\lambda_c \equiv 0$ and $\lambda_p \equiv 0$. This gives us a contradiction because the pair (λ, λ^0) must be non-zero. By homogeneity of the Hamiltonian, we may then assume that $\lambda^0 = -1$. The Hamiltonian condition in Pontryagin's Principle then gives

$$u(t) \in \operatorname{argmax}_{v\in[0,1]} H(x(t), \lambda(t), -1, v) \quad \text{a.e. } t \in [0, T]. \tag{8}$$

An extremal is a triplet $(x(\cdot), \lambda(\cdot), u(\cdot))$ satisfying (2)-(6)-(8) (since $\lambda^0 \neq 0$, we thus only consider normal extremals in the sequel). From (8), the control law is given by the sign of the *switching function*

$$\phi := \lambda_p k_R c(1-c-p),$$

which gives

$$\begin{cases} \phi(t) > 0 \;\Rightarrow\; u(t) = 1, \\ \phi(t) < 0 \;\Rightarrow\; u(t) = 0. \end{cases} \tag{9}$$

A Bang+ arc (resp. Bang−) is a portion of trajectory defined over some time interval $[t_1, t_2]$ such that $u = +1$ (resp. $u = 0$) over $[t_1, t_2]$. The next property shows that any optimal control is necessarily of type Bang+ in some neighborhood of $t = T$.

Proposition 2. *If u is an optimal control of* (P)*, there exists $\tau \in [0, T)$ such that one has $u(t) = +1$ for every $t \in [\tau, T]$.*

Proof. At time $t = T$, one has $\phi(T) = 0$. In addition, by differentiating ϕ w.r.t. t we find

$$\dot{\phi}(T) = -k_R c(T)(1 - c(T) - p(T))v_P'(p(T)) < 0$$

using $\lambda_c(T) = \lambda_p(T) = 0$. By continuity, there exists $\tau \in [0, T)$ such that one has $\phi > 0$ over $[\tau, T)$ implying the desired property. □

The switching function ϕ may also vanish over a sub-interval $[t_1, t_2] \subset [0, T]$. If this happens, we say that the extremal is *singular* over $[t_1, t_2]$ and that a singular arc occurs. The singular arc is the portion of the corresponding trajectory over $[t_1, t_2]$. As we shall next see, such arcs have a significant impact on the optimal synthesis, that is why, we now study more into details their properties.

4.2. Study of singular arcs

In this section, we provide properties of singular arcs such as Legendre-Clebsch's condition that will allow us to have an insight into optimal paths. Recall that, given an optimal trajectory $(c(\cdot), p(\cdot))$ associated with a control $u(\cdot)$, along any singular arc defined over a time interval $[t_1, t_2]$, the inequality

$$\frac{\partial}{\partial u}\frac{d^2 H_u}{dt^2} \geq 0 \tag{10}$$

should be fulfilled over $[t_1, t_2]$. Inequality (10) expresses the second order necessary optimality condition (Legendre-Clebsch's condition). In particular, if (10) fails to hold, no singular arc occurs. In order to check if (10) is fulfilled, note that $\frac{\partial}{\partial u}\frac{d^2 H_u}{dt^2}$ coincides with $\ddot{\phi}_{|u} := \frac{\partial}{\partial u}\ddot{\phi}$.

Lemma 3. *Along any singular arc defined over a time interval $[t_1, t_2]$, one has:*

$$\lambda_c = \frac{-v_P'(p)}{k_R c + v_P'(p)(1 - c)} \text{ and } \dot{\lambda}_c = \frac{-v_P'(p)(v_P(p) + k_R(1 - 2c - p))}{k_R c + v_P'(p)(1 - c)}. \tag{11}$$

Proof. Along a singular arc defined over a time interval $[t_1, t_2]$, one has $\phi \equiv 0$ over $[t_1, t_2]$, thus $\lambda_p \equiv 0$ as well as $\dot{\lambda}_p \equiv 0$. By differentiating λ_p and using (6), we find the desired expressions of λ_c as well as $\dot{\lambda}_c$ along $[t_1, t_2]$. □

Proposition 3. *Along any singular arc defined over a time interval* $[t_1, t_2]$*, the Legendre-Clebsch condition* (10) *is fulfilled with a strict inequality.*

Proof. Recall that along a singular arc $\lambda_p \equiv 0$. By differentiating ϕ w.r.t. t over $[t_1, t_2]$, we thus get

$$\dot{\phi} = -k_R c(1-c-p)(k_R c\lambda_c + v_P'(p)(1-c)\lambda_c + v_P'(p)).$$

Now, when differentiating $\dot{\phi}$ w.r.t. t, the terms involving explicitly the control u come from the derivate of the function $t \mapsto v_P'(p(t))$ w.r.t. t. Hence, along a singular arc, we find that

$$\begin{aligned}\ddot{\phi}_{|u} &= -k_R c(1-c-p)v_P''(p)((1-c)\lambda_c + 1)\dot{p}_{|u} \\ &= -\frac{k_R^2 c^2(1-c-p)v_P''(p)}{k_R c + v_P'(p)(1-c)}\dot{p}_{|u} \\ &= -\frac{k_R^3 c^3(1-c-p)^2 v_P''(p)}{k_R c + v_P'(p)(1-c)},\end{aligned}$$

where the second equality follows from (11). Observe that the quantity $k_R c + v_P'(p)(1-c)$ is positive. Since v_P is strictly concave, $v_P'' < 0$, and we deduce that $\ddot{\phi}_{|u} > 0$. The result follows. □

Remark 1. (i) *The fact that Legendre-Clebsch's condition is fulfilled indicates that the optimal synthesis may exhibit a singular arc (although the occurrence of such an arc also depends on the initial condition). If a singular arc occurs, such an arc is usually called a turnpike (see, e.g., Boscain and Piccoli (2004) or Bayen et al. (2018)) meaning that during a certain time interval, the optimal control must take intermediate values between* 0 *and* 1 *(see Proposition 4). According to turnpike properties (see Trélat and Zuazua (2015) and references herein), the corresponding portion of trajectory should then remain close to an optimal steady state point as computed in Section 3.*

Remark 2. *The strict concavity of* v_P *is fundamental to ensure Legendre-Clebsch's condition.*
(i) *If a linear expression is used* ($v_P'' = 0$)*, then* $\dot{\phi}_{|u}$ *would be zero implying the possible occurrence of a singular arc of second order (see Mairet and Bayen (2020)), i.e., the singular control cannot be computed from* $\ddot{\phi}$ *(as in Proposition 4), but from* $\dddot{\phi}$*.*
(ii) *If a Hill-type expression is used (see, e.g., Moser (1958)) and if the*

optimal steady-state is such that p^* lies in the convex part of the curve $v_P(\cdot)$, Legendre-Clebsch's condition is not satisfied in a neighborhood of p^*. Thus, it can be expected that no singular arc occurs in that case. This issue is further investigated in Appendix A.

We now provide the expression of the singular control as a feedback of the state.

Proposition 4. *Along a singular arc defined over a time interval $[t_1, t_2]$, the singular control $t \mapsto u_s(t)$ is given by $u_s(t) := \psi(c(t), p(t))$, $t \in [t_1, t_2]$ where $\psi : \Omega \to \mathbb{R}$ is defined as*

$$\psi(c,p) := -\frac{a(c,p)}{b(c,p)},$$

with

$$\begin{aligned} a(c,p) &:= -k_R\left(cpv_P(p)v_P''(p) + v_P'(p)[v_P'(p)((1-c)^2-p) + v_P(p) - k_Rc^2]\right), \\ b(c,p) &:= k_R^2c^2(1-c-p)v_P''(p). \end{aligned} \tag{12}$$

Proof. Since $\lambda_p = \dot{\lambda}_p = 0$ over $[t_1, t_2]$, we find that

$$\begin{aligned} &\ddot{\phi} = k_Rc(1-c-p)\ddot{\lambda}_p \\ &= -k_Rc(1-c-p)\left[\dot{\lambda}_c[v_P'(p)(1-c) + k_Rc] + \lambda_c\frac{d}{dt}[v_P'(p)(1-c) + k_Rc] + v_P''(p)\dot{p}\right] \end{aligned} \tag{13}$$

Now, putting (11) into the previous expression and collecting the terms with u (coming from $\dot{p}$) and the ones without u allows to write (13) as

$$\ddot{\phi} = -\frac{k_Rc(1-c-p)}{k_Rc + v_P'(p)(1-c)}(a(c,p) + b(c,p)u),$$

where a, b are given by (12). Using that $\ddot{\phi} = 0$ over $[t_1, t_2]$, the result follows. □

Remark 3. *To complete the sign condition* (9) *coming from the Hamiltonian condition* (8)*, the previous proposition implies that if $\phi \equiv 0$ over some time interval $[t_1, t_2]$, then the corresponding singular path necessarily coincides with a portion of orbit of*

$$\left|\begin{array}{ll} \dot{c} &= v_P(p)(1-c) - k_Rc(1-c-p), \\ \dot{p} &= -\frac{a(c,p)}{b(c,p)}k_Rc(1-c-p) - pv_P(p), \end{array}\right. \tag{14}$$

that is, system (2) *in which the input u is the feedback control $u = \psi(c,p)$.*

We now analyze the asymptotic behavior of the dynamical system (14) near (c^*, p^*).

Proposition 5. *The optimal steady-state point (c^*, p^*) is a saddle point of (14).*

Proof. First, note that system (14) can be equivalently rewritten

$$\left| \begin{array}{ll} \dot{c} & = v_P(p)(1-c) - k_R c(1-c-p), \\ \dot{p} & = \frac{v_P'(p)}{c v_P''(p)}(v_P'(p)[(1-c)^2 - p] + v_P(p) - k_R c^2) \end{array} \right. \tag{15}$$

Recall that the optimal steady-state point satisfies $p^* = (u^*)^2 = (1-c^*)^2$, $c^* = 1-u^*$ where u^* is the unique solution of the equation $v_P(u^2) = k_R(1-u)^2$ over $[0,1]$. Thanks to these relations, we can verify that (c^*, p^*) is an equilibrium of (15). In addition, the Jacobian matrix of (15) at this point writes

$$A := \left[\begin{array}{cc} \alpha & \beta \\ \gamma & \delta \end{array} \right],$$

with

$$\left| \begin{array}{ll} \alpha & = -v_P(p^*) - k_R(1 - 2c^* - p^*), \\ \beta & = v_P'(p^*)(1-c^*) + k_R c^*, \\ \gamma & = -\frac{2v_P'(p^*)}{c^* v_P''(p^*)}(v_P'(p^*)(1-c^*) + k_R c^*), \\ \delta & = -\frac{v_P'(p^*)}{c^*}((1-c^*)^2 - p^*). \end{array} \right.$$

We see that $\beta > 0$ and that $\gamma > 0$, and thanks to the definition of (c^*, p^*), we verify that $\alpha = \delta = 0$. It follows that the matrix A has exactly two non-zero eigenvalues of opposite sign which ends the proof. □

At this step, we have seen that an optimal control satisfies almost everywhere over $[0, T]$: either $u \in \{0, 1\}$ (depending on the sign of ϕ), or u is singular and its expression u_s is provided by Proposition 4. Observe that there is no guarantee that along a singular arc, the singular arc is *admissible*, i.e.,

$$|u_s| \leq 1. \tag{16}$$

Indeed, the value of the singular control $u_s = \psi(c, p)$ provided by the Pontryagin Maximum Principle may exceed the bounds on the control u. Nevertheless, when the singular arc is close to the optimal steady-state point, then inequality (16) is fulfilled as we shall next see.

Property 1. *There exists a neighborhood $\mathcal{V} \subset \Omega$ of (c^*, p^*) such that one has $|\psi(c,p)| \leq 1$ for every $(c,p) \in \mathcal{V}$.*

Proof. When $(c,p) \to (c^*, p^*)$, one has

$$\psi(c,p) \sim -\frac{k_R c^* p^* v_P(p^*) v_P''(p^*)}{k_R^2 (c^*)^2 (1-c^*-p^*) v_P''(p^*)} = -\frac{p^* k_R (c^*)^2}{k_R c^* (1-c^*-p^*)}$$

using that $v_P(p^*) = k_R (c^*)^2$ in the above equality. This gives

$$|\psi(c,p)| \sim \frac{c^* p^*}{1-c^*-p^*} = 1 - c^*,$$

using $p^* = (1-c^*)^2$ and the result follows since $c^* \in (0,1)$. □

So, we can conclude about the admissibility of a singular arc when the corresponding trajectory is sufficiently close to the saddle point (c^*, p^*).

4.3. Discussion about optimal trajectories

The saddle point property of (c^*, p^*) along the singular arcs is crucial in order to understand the behavior of optimal paths and it is in line with properties of turnpikes as in Trélat and Zuazua (2015). The optimal point (c^*, p^*) possesses a stable and unstable one-dimensional manifold. Hence, an optimal trajectory can take advantage of the stable manifold to approach (c^*, p^*) which by definition is the point for which production is optimal at steady-state. Because of the transversality conditions (recall that on optimal path contains a Bang + arc over some time interval $[T-\varepsilon, T]$), an optimal trajectory will leave a neighborhood of (c^*, p^*) taking advantage of the unstable manifold before switching to $u = +1$ until the terminal time.

Thanks to these qualitative properties, we can expect an optimal path to be of the following type:

$$\gamma_1 - \gamma_s - \gamma_2, \tag{17}$$

where γ_s is a singular arc, and γ_i, $i = 1, 2$ is the union of (possibly a few) Bang arcs.

- The first part γ_1 allows an optimal path to approach $\mathcal{V}$ before switching to a singular arc.
- Along the singular arc γ_s, the trajectory stays close to the optimal steady-state.

- In the third part γ_2, the trajectory moves away from the optimal steady-state point. For our biological problem, this last transient corresponds to an artifact due to a fixed final time (recall (7)), and only the transition from the initial condition to the optimal steady-state is relevant.

4.4. Numerical optimal solutions

In this section, we solve numerically the optimal control problem (P) by a direct method using the software `bocop` v.2.1.0 (Team Commands, Inria Saclay, 2017; Bonnans et al., 2017). This will corroborate the structure of an optimal control given by (17). A time discretization allows to transform the optimal control problem into a nonlinear optimization problem, solved here by interior point techniques. A discretization by a Lobatto IIIC formula (6th order) was used with 400 time steps, and the relative tolerance for NLP solver was set at 10^{-10}. We consider a Michaelis-Menten function (1) for the photosynthetic rate, a light intensity I =100 μmol.m^{-2}.s^{-1}, and the following parameter values: k_P =1.6 d^{-1}, k_R =2.1 d^{-1}, and K =140 μmol.m^{-2}.s^{-1}.

The optimal trajectories obtained numerically are composed of two bang arcs followed by a singular arc (which approaches the optimal steady state), see Fig. 3. These numerical results tend to confirm our conjecture about the structure of an optimal solution given by (17) : the optimal strategy corresponds to a turnpike behavior. Additionally, these results show the reliability of the numerical method. Trajectories are actually computed by the direct method, without any knowledge of the theoretical solution, and the numerical solutions present several characteristics demonstrated previously, such as the singular arc approaching to the optimal steady state (see Fig. 4).

5. Model fitting: a bi-level optimization problem

Several microbial models with dynamic resource allocation have been proposed recently, but comparison with experimental data is rarely carried out. In this context, we propose a numerical method to estimate model parameters from experimental data and finally evaluate if our framework allows to represent quantitatively microalgal photoacclimation dynamics. A light down-shift is used as a case study. After a long acclimation to a light intensity I^-, microalgae are shifted at $t = 0$ to a different intensity I.

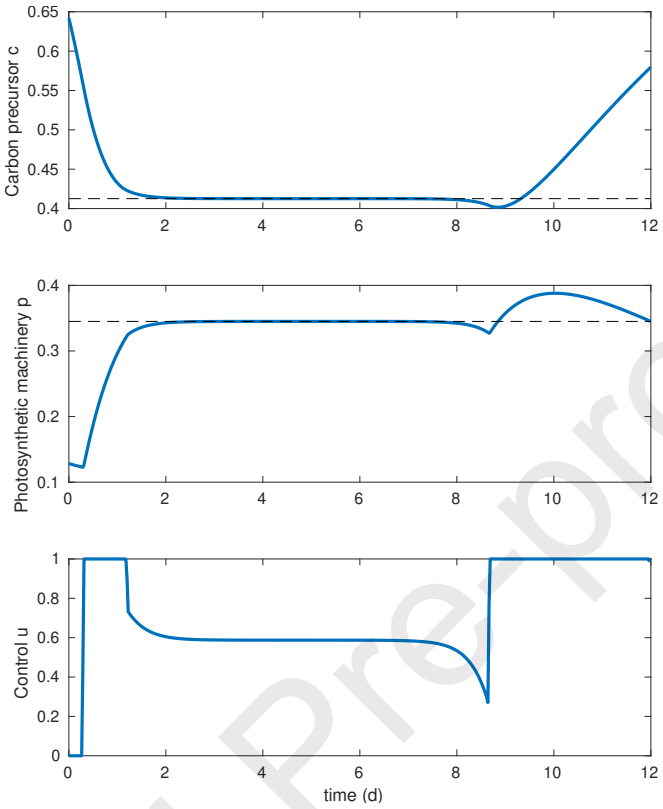

Figure 3: Optimal trajectory (solution of (P)), obtained numerically by the direct method using the `bocop` solver (Team Commands, Inria Saclay, 2017). The black dashed lines correspond to the optimal steady-state.

5.1. Problem formulation

The model outputs y is a function g of the states $x = (c, p)$ and also possibly of the parameters θ, *i.e.*

$$y(t) = g(x(t), \theta),$$

We consider a set of measurements $\bar{y}_k \in \mathbb{R}^m$, corresponding to time instants $t_1, \ldots, t_{n_k}$, $k \geq 1$. Our objective is to find the set of parameters $\theta = (k_P, k_R, K)^T \in (0, +\infty)^3$ such that the optimal solution $x(\cdot)$ of (P) fits

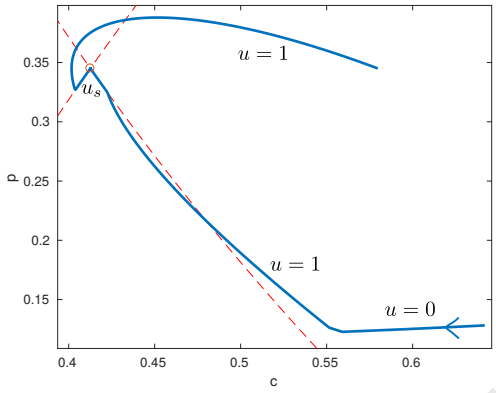

Figure 4: Plot of an optimal path (blue line) in the plane (c, p) by the direct method : in the first phase, the trajectory approaches (c^*, p^*) (red dot) ; in the second one, it remains close to it along a singular arc (red dashed lines) ; to satisfy transversality conditions it finishes with a single Bang+ arc.

the experimental data. This leads to a so-called *bi-level optimization problem*:

$$\min_{\theta \in C} \sum_k \left(g(x^\star(t_k), \theta) - \bar{y}_k\right)^T Q \left(g(x^\star(t_k), \theta) - \bar{y}_k\right)$$
$$\text{s.t.} \left| \begin{array}{ll} u^\star & \in \operatorname{argmax}_{u \in \mathcal{U}} \int_0^T v_P(p(t))\, \mathrm{d}t, \\ \dot{x}(t) & = f(x(t), u(t), \theta) \quad \text{a.e. } t \in [0, T], \\ x(0) & = x^*(I^-, \theta), \end{array} \right. \tag{18}$$

where $Q \in \mathcal{M}_{n_k}(\mathbb{R})$ is a square weighting matrix, C is a non-empty compact subset of $(0, +\infty)^3$, $f(\cdot, \cdot, \cdot)$ is the dynamics given by System (2) (in which we incorporate the dependency w.r.t. the parameters), $x^\star$ is the solution to this system associated with $u^\star \in \mathcal{U}$. In addition, the initial condition is $x^*(I^-, \theta)$ which is the optimal steady-state point as computed in Lemma 2, and which depends on the light intensity and parameters. Problem (P) plays the role of *lower level program* whereas the optimization w.r.t. θ in (18) is the *upper level program*. Problem (18) is unusual because it couples an optimal control problem to a non-linear program.

Experimental data with the microalga *Dunaliella tertiolecta* (Sukenik et al., 1990) have been considered. After several days of acclimation at 700 μmol.m^{-2}.s^{-1}, light intensity has been shifted down to 70 μmol.m^{-2}.s^{-1} at $t = 0$. The following measurements have been used for parameter estimation:

- The relative content of LHCII, determined from Western blots. We consider that the photosynthetic sector p follows the same relative dynamics as this protein, so we compare these measurements with $p(t)/p(0)$.

- The photosynthetic rate (v_P), given in mole C.cell^{-1}.s^{-1} and converted in d^{-1} assuming a carbon content of 3.5 pmole C.cell^{-1} (determined by equilibrium values at low light). It actually corresponds to a carbon specific growth rate.

- The specific growth rate, which was calculated from cell measurements. We assume that the cellular dynamics is driven by the macromolecule content, and so the cellular growth rate corresponds in our model to the macromolecule synthesis rate per unit of macromolecule $v_R/(p+r)$. To avoid confusion with the photosynthetic rate, we call it *macromolecule growth rate*.

5.2. Numerical method

The solution of the bi-level optimization problem (18) is determined using a classical direct search routine (by the Levenberg-Marquardt method with the `lmfit` package in `Python` (Newville et al., 2014)). At each iteration, the `bocop` solver is called to solve the lower level problem for a given θ, using as initial condition the optimal steady-state (which depends on θ) for the light intensity of pre-acclimation. We take 100 time steps, with a time horizon large enough such that the trajectory moves away from the optimal equilibrium after the last measurement (this final dynamics is not relevant in our biological problem). For each variable, the square errors between the measurements and the optimal trajectory are weighted by the inverse of the square of the measurement mean. The computation time to solve the bi-level optimization problem on a classical laptop was approximatively one minute. Finally, we use in a second step a Markov Chain Monte Carlo (MCMC) method to better assess parameter uncertainty, see Appendix B.

5.3. Fitting results

The estimated parameters with their confidence interval are given in Table 1. The optimal trajectory is shown with the experimental data in Fig. 5. The fitted optimal trajectory represents well the dynamics of photoacclimation. The photosynthetic rate falls sharply at $t = 0$ with the light down-shift, and then slowly increases with the reallocation of resources to the photosynthetic

sector. On the other hand, the macromolecule growth rate slowly decreases after the light shift, until reaching the new steady-state. The good model fit is the first hint that our approach is effective, and it should now be validated with other experiments. The parameter confidence regions shown in Appendix B indicate that k_p and K - the two parameters defining the photosynthetic rate - are correlated. More experimental data would be necessary to better estimate these parameters.

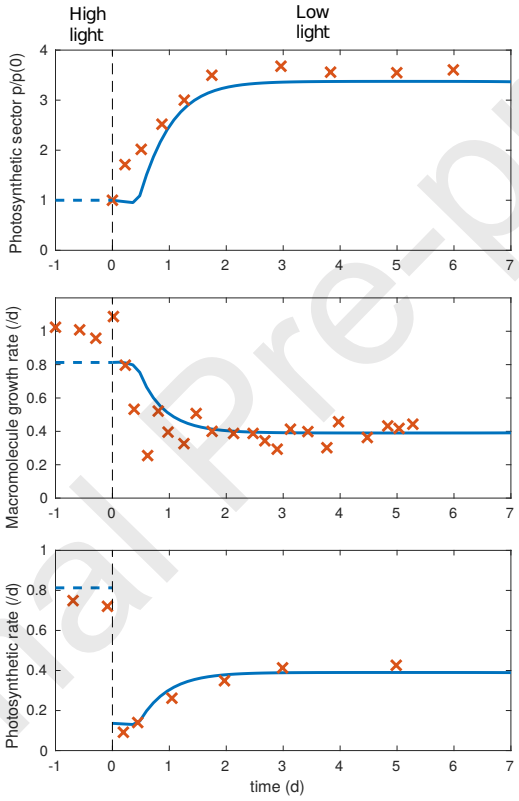

Figure 5: Trajectory corresponding to the solution of the bi-level optimization problem (18). The model (blue lines) fits the experimental data (red crosses) of the microalga *Dunaliella tertiolecta* facing a light intensity down-shift from 700 μmol.m^{-2}.s^{-1} to 70 μmol.m^{-2}.s^{-1} at $t = 0$ (Sukenik et al., 1990).

Table 1: Parameters (with their confidence intervals) estimated as the solution of the bi-level optimization problem (18)

Parameter	Definition	Value	Unit
k_P	Maximum photosynthetic rate	1.81 ± 0.34	d^{-1}
k_R	Macromolecule synthesis rate constant	1.52 ± 0.14	d^{-1}
K	Half saturation constant for photosynthesis	62.1 ± 25.0	$\mu\mathrm{mol.m}^{-2}.\mathrm{s}^{-1}$

6. Optimal allocation under day/night cycles

6.1. Problem formulation

Given that microalgae have evolved under day-night cycles, one may assume that they have an optimal allocation strategy to deal with these conditions. In this context, we wish to determine with our coarse-grained model the optimal trajectory under such a day/night cycle, by imposing that the initial condition is equal to the final condition (the cycle can thus be repeated day after day). This gives the following optimal periodic control problem:

$$\max_{u(\cdot)\in\mathcal{U}} J(u) := \int_0^T v_P(p(t), I(t))\,\mathrm{d}t, \;\; \text{s.t. } (c(0), p(0)) = (c(T), p(T)), \qquad (19)$$

where $(c(\cdot), p(\cdot))$ is the unique solution of (2) for a given control $u \in \mathcal{U}$, and $T = 1$ d. For the light pattern, we use a night period τ followed by a sinusoidal signal:

$$I(t) := \left| \begin{array}{ll} 0 & \text{for} \quad 0 \leq t \leq \tau, \\ I_{\max} \sin^2\left(\frac{t-\tau}{T-\tau}\pi\right) & \text{for} \quad \tau < t \leq T. \end{array} \right.$$

Note that in Problem (19), the initial condition is unknown since a periodic constraint on the state has been added. In line with Hernández Limón et al. (2020), we use $I_{\max} = 1000$ $\mu\mathrm{mol.m}^{-2}.\mathrm{s}^{-1}$ and $\tau = 0.46$ d.

6.2. Numerical simulations reveal an anticipatory behavior

Using our fitted model, optimal allocation strategy under day/night cycles is determined numerically using the direct method with `bocop` (as done previously in Section 4). Results are presented in Fig. 6. The optimal trajectory consists in three Bang arcs and the corresponding control u equals to

0-1-0. Note that several simulations with different parameter values and light signals (changing the maximum light intensity and the day length) have been carried out, and the structure of the optimal trajectory remains the same. Interestingly, the synthesis of the photosynthetic apparatus always begins a few hours before dawn in our predictions. This behavior is actually observed in several laboratory and field studies, see *e.g.*, Zinser et al. (2009); John et al. (2012); Hernández Limón et al. (2020). The gene expression pattern of the photosynthetic sector measured in the latter study has been plotted in Fig. 6 to show the consistency with our predictions. Microalgae show thus an anticipation capacity - based a priori on their circadian clock (Mittag, 2001; Suzuki and Johnson, 2001) - which allows them to deal with the day/night cycle optimally according to our assumptions.

6.3. Mathematical insights on the day/night problem

Some explanation of the optimal trajectory structure (*i.e.*, bang arcs 0-1-0) can be obtained using the Pontryagin Maximum Principle (PMP). First, even though (2) is non-autonomous (because v_P explicitly depend on time), the Hamiltonian system (2)-(6) remains unchanged. Because of the periodicity condition on the state, it is now supplemented with the periodic condition $\lambda(0) = \lambda(T)$ on the adjoint state. It follows that the switching function ϕ whose sign gives the value of an optimal control (excepting along singular arcs) satisfies

$$\phi(0) = \phi(T).$$

Hence, whenever $\phi(0) \neq 0$, there is $\varepsilon > 0$ such that $u \equiv 1$ or $u \equiv 0$ over $t \in [0, \varepsilon] \cup [T - \varepsilon, T]$. So, the PMP shows that an optimal control takes the same value near $t = 0$ and $t = T$ unless $\phi(0) \neq 0$. We also infer that no singular arc occurs over a time interval $[\tau - \eta, \tau + \eta]$ because of the asymmetry of light intensity $I(\cdot)$ defining v_P. The fact that an optimal periodic control has a "low" number of switching times is in line with some recent papers about periodic optimal control problems such as Bayen et al. (2020) in which the structure 0-1-0 is proved to be optimal.

A complete study of qualitative properties of (19) via the PMP should deserve future work: in particular, the questions of existence and attractivity of periodic solutions to (2) or the exclusion of singular arcs in the periodic setting as in Bayen et al. (2020).

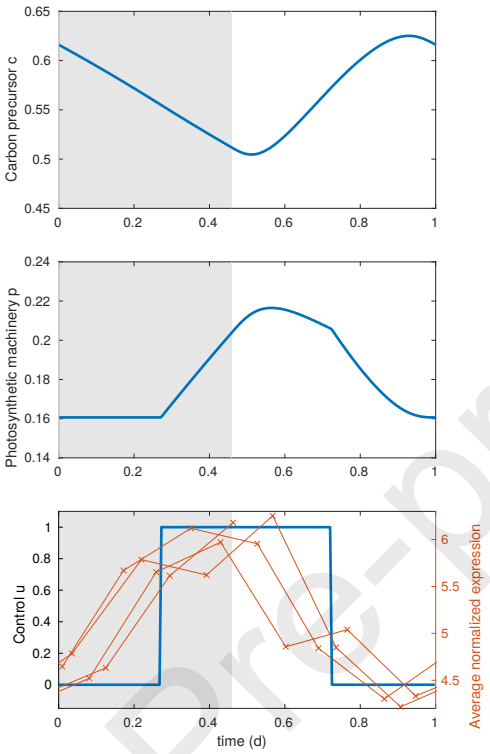

Figure 6: Optimal trajectory obtained numerically by the direct method using the `bocop` solver under day-night cycle. The control u (bottom figure, blue line, left axis), corresponding to the allocation of macromolecule synthesis to the photosynthetic apparatus, is switched on a few hours before dawn. This anticipatory behavior is in line with the averaged normalized expression of genes involved in photosynthesis in *Emiliania huxleyi* in the North Pacific Subtropical Gyre (Hernández Limón et al., 2020) (bottom figure, red marks, right axis).

7. Discussion

7.1. From mathematical analysis to biological insights

A coarse-grained model was proposed to predict microalgae growth and photoacclimation dynamics. Based on evolutionary principle, growth can be represented by an optimization problem: intracellular resources should be allocated in order to maximize microalgae growth over a time period. The optimal control problem was first studied with the Pontryagin Maximum Principle. Facing a light shift, we have shown that the optimal strategy of photoacclimation is a turnpike: after a transient, the trajectory remains close

to the optimal steady state. Numerical results were in line with our analysis, confirming our development and the reliability of the numerical method. Model parameters were then estimated by solving a bi-level optimization problem. Finally, we have studied the problem of photoacclimation under day-night cycles, mainly through numerical simulations.

From a biological point of view, the proposed model captures the trend of steady-state photoacclimation, *i.e.*, the photosynthetic apparatus content decreases with light intensity. Additionally, the model fits well photoacclimation dynamics when microalgae face a light down-shift. More surprising, the model also represents - at least qualitatively - the anticipation behavior of microalgae under day-night cycle: the synthesis of the photosynthetic apparatus starts a few hours before dawn, as observed experimentally in laboratory and field studies (Zinser et al., 2009; John et al., 2012; Hernández Limón et al., 2020).

7.2. Predicting anticipatory behavior

Several photoacclimation models have been proposed, where the allocation to the photosynthetic apparatus is either empiric (*i.e.*, defined as a function of environmental conditions) (Geider et al., 1998; García-Camacho et al., 2012; Bernard et al., 2015; Nikolaou et al., 2016; Straka and Rittmann, 2018) or based on optimization principle (Shuter, 1979; Armstrong, 2006; Geider et al., 2009; Jahn et al., 2018; Faizi and Steuer, 2019; Zavřel et al., 2019). But, to our knowledge, only our approach allows to represent the anticipatory behavior of algae.

More generally, the anticipation capacity of microorganisms have been observed, *e.g.* in the bacteria *Escherichia coli* and the yeast *Saccharomyces cerevisiae* (Mitchell et al., 2009). To represent anticipatory behavior with optimization-based models, optimization over a time window is necessary given that the biological response starts before the environmental signal. A notable example of cellular anticipation was proposed by Waldherr et al. (2015) who predicted a change of gene expression before the complete depletion of a nutrient. On the other hand, anticipation is possible only in some conditions, *e.g.*, under periodic regime or if a signal announces a change of environmental conditions, and only if the species have evolved in these conditions. In consequence, optimization over a time period could not be used in any cases.

7.3. Fitting resource allocation models

On a methodological aspect, the originality of this work is to propose a fitting procedure for dynamic resource allocation models, leading to a bi-level optimization problem in which the lower level is an optimal control problem and the upper one is a standard non-linear program.

A few studies have deal with this kind of problem, in particular to estimate the objective function that a biological system optimizes (the so-called inverse optimal control problem). This objective function is generally written as a weighted sum of known functions, and one aims at estimating the weights (leading to a parameter estimation problem). Such a problematic has been encountered in the context of motion planning. For instance, Mombaur et al. (2010) have identified the underlying optimality criteria of human locomotion. The solution was obtained with two optimization algorithms, where the upper level calls at each iteration the lower level. In Albrecht et al. (2012), a bilevel problem was also formulated to tackle arm movement. It was solved numerically by a discretization method and the use of optimality conditions in non-linear programming.

Closer to our study, Tsiantis et al. (2018) have proposed a computational approach to solve inverse optimal control problem in systems biology. As a first step, the inputs and parameters (corresponding respectively to $u(t)$ and θ with our notation) are estimated by minimizing the error between measurements and model outputs. The resulting parameters are then used to compute the Pareto set of optimal control. Finally, the objective function is estimated such that the optimal trajectory corresponds to the observed dynamics. The major advantage of this approach is that there is no longer a bi-level optimization problem, but identifiability issues are nevertheless to be feared when estimating the input.

The numerical methods proposed here and in the aforementioned studies work on relatively small models (with a limited number of variables), but new developments will be required for bigger models (*i.e.*, for metabolic models at genome scale). Finding issues in a general setting to this kind of optimization problems could also be investigated in future works.

Code availability

Codes for simulation with `bocop` (v.2.1.0) under constant light and day-night cycle are available at https://github.com/fmairet/photoacclimation. Code for parameter estimation will be made available upon request.

Declaration of Competing Interest

The authors declare that they have no known competing financial interests or personal relationships that could have appeared to influence the work reported in this paper.

Acknowledgement

This research benefited from the support of the FMJH Program PGMO and from the support to this program from EDF-THALES-ORANGE. We are grateful to Walid Djema for fruitful exchanges about singular arcs and to Pierre Martinon for his help with `bocop`.

Appendix A. Simulations with other kinetics rates

In this appendix, we investigate if our results are still valid with other expressions for the kinetics rates. In particular, we have computed optimal trajectories with `bocop`, as done in Section 4.4, with two modifications of the model.

Appendix A.1. Hill's function for the photosynthetic rate

In the main article, we considered an increasing concave function for the photosynthetic rate. This encompasses the majority of models found in the literature, but Hill's expressions are sometimes used (*e.g.*, in Grima et al. (1994)). The photosynthetic rate becomes:

$$v_P(p, I) = k_P \frac{(pI)^n}{K^n + (pI)^n}.$$

In this case, our convexity hypothesis - used to check the optimality of the singular arc (Legendre-Clebsch's condition, see Section 4.2) - is not satisfied. If light intensity is high enough, the optimal steady-state is such that p^* is in the concave part of the curve, so the turnpike strategy is optimal. On the other hand, if light intensity is low, the optimal steady-state is such that p^* lies in the convex part of the curve. In consequence, Legendre-Clebsch's condition is not satisfied and the optimal trajectory is a concatenation of bang arcs (no singular arc occurs). Numerical simulations with `bocop` show that in this case, the optimal trajectory oscillates around the optimal steady-state (see Fig. A.7 for a simulation with I =160 μmol.m^{-2}.s^{-1}, and the following

parameter values: k_P =1.6 d^{-1}, k_R =2.1 d^{-1}, K =140 μmol.m^{-2}.s^{-1}, and n =5). We thus obtain a different behavior, even if the oscillations remain rather weak. It would therefore be interesting first of all to look more into details at the relevance of using this kind of kinetic rate for photosynthesis, and then possibly to deepen the question.

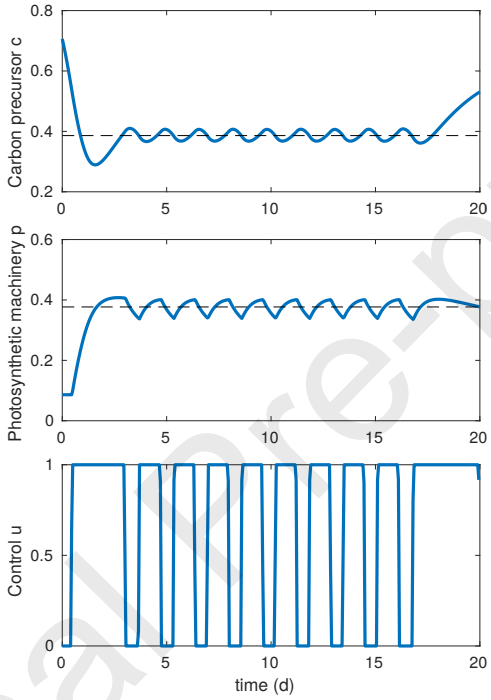

Figure A.7: Optimal trajectory (solution of (P)) when considering a Hill function for the photosynthetic rate. The black dashed lines correspond to the optimal steady-state.

Appendix A.2. Michaelis-Menten function for the macromolecule synthesis rate

As a second variation of the model, we use Michaelis-Menten function for both the photosynthetic rate and the macromolecule synthesis rate:

$$v_P(p, I) = k_P \frac{pI}{K + pI}, \quad \texttt{and} \quad v_R(c, r) = k_R \frac{c}{K_R + c} r.$$

We have performed numerical simulations with various parameter sets. In that case, the optimal strategy remains the same as in Section 4.4, *i.e.*, the

turnpike strategy. See Fig. A.8 for an example with I =60 μmol.m^{-2}.s^{-1}, and the following parameter values: k_P =1.6 d^{-1}, k_R =2.1 d^{-1}, K =80 μmol.m^{-2}.s^{-1}, and K_R =0.1. Thus, it seems that our results still hold for more general expressions for the macromolecule synthesis rate.

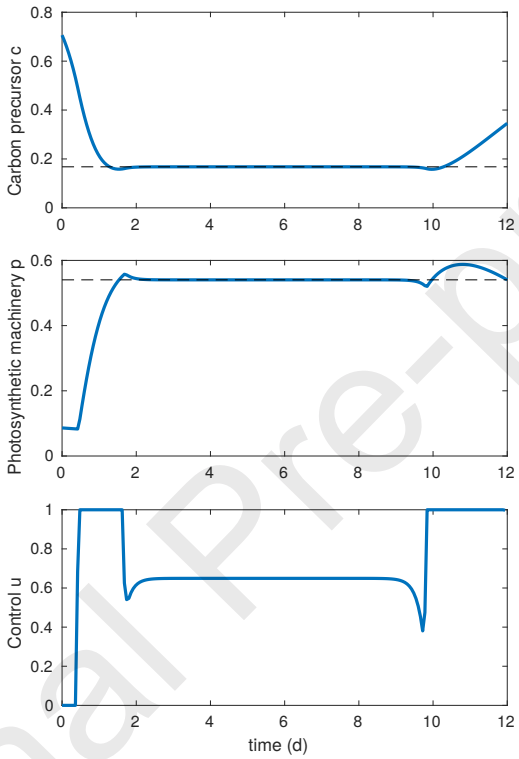

Figure A.8: Optimal trajectory (solution of (P)) when considering a Michaelis-Menten function for the macromolecule synthesis rate. The black dashed lines correspond to the optimal steady-state.

Appendix B. Evaluation of parameter uncertainty

We explore the parameter space around the optimal solution to get a better insight on parameter uncertainty. To do so, we use the affine-invariant ensemble sampler for MCMC `emcee` (Foreman-Mackey et al., 2013), implemented in the `lmfit` package (Newville et al., 2014). Figure B.9 shows the two dimensional projections of the posterior probability distributions of the

parameters. It appears that the two parameters k_p and K (which define the photosynthetic rate) are correlated. Finally, we also randomly took 50 samples from the chain to illustrate the effect of parameter uncertainty on model predictions. All the associated trajectories follow the trends of the data (see Figure B.10). Note however that the model slightly underestimates the photosynthetic apparatus sector just after the light down-shift.

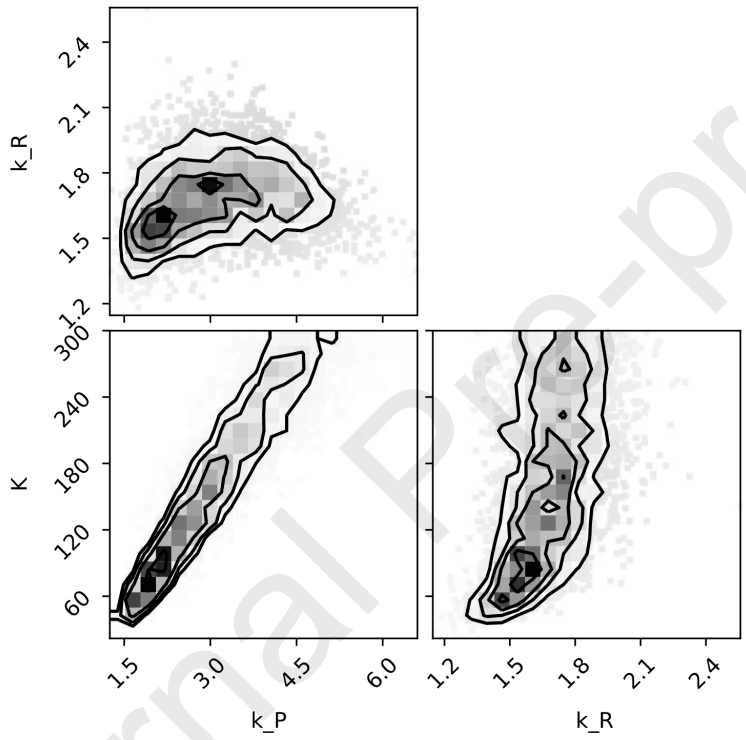

Figure B.9: Pairwise posterior distribution of model parameters, obtained with a MCMC algorithm.

References

Albrecht, S., Leibold, M., Ulbrich, M., 2012. A bilevel optimization approach to obtain optimal cost functions for human arm movements. Numerical Algebra, Control and Optimization 2, 105–127.

Armstrong, R., 2006. Optimality-based modeling of nitrogen allocation and

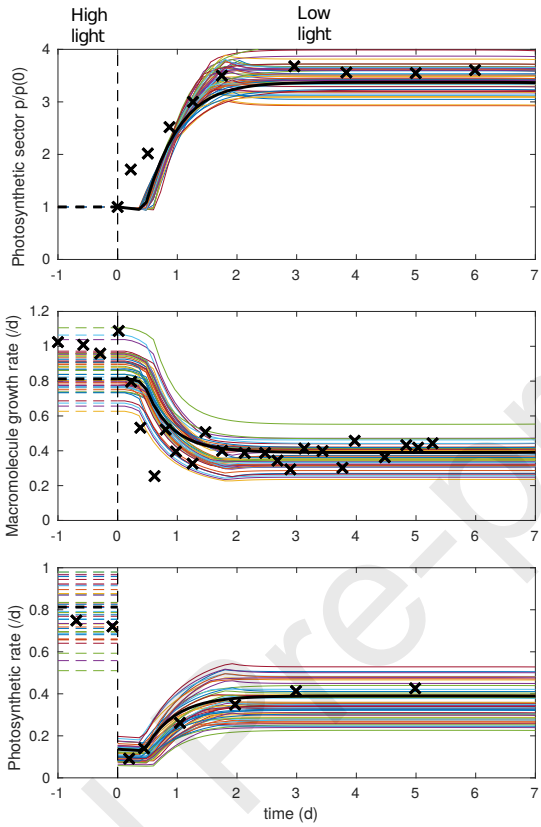

Figure B.10: Trajectories from the MCMC approach. The black line corresponds to the best fit.

photoacclimation in photosynthesis. Deep Sea Research Part II: Topical Studies in Oceanography 53, 513–531.

Bayen, T., Cots, O., Gajardo, P., 2018. Analysis of an Optimal Control Problem Related to the Anaerobic Digestion Process. J. Optim. Theory Appl. 178, 627–659. doi:10.1007/s10957-018-1292-7.

Bayen, T., Tani, F.Z., Rapaport, A., 2020. Optimal periodic control for scalar dynamics under integral constraint on the input. Mathematical Control & Related Fields 10, 547–571.

Bernard, O., Mairet, F., Chachuat, B., 2015. Modelling of microalgae cul-

ture systems with applications to control and optimization, in: Microalgae Biotechnology. Springer, pp. 59–87.

Bonnans, Frederic, J., Giorgi, D., Grelard, V., Heymann, B., Maindrault, S., Martinon, P., Tissot, O., Liu, J., 2017. Bocop A collection of examples. Technical Report. INRIA. URL: `http://www.bocop.org`.

Boscain, U., Piccoli, B., 2004. Optimal syntheses for control systems on 2-D manifolds. volume 43 of *Mathématiques & Applications (Berlin) [Mathematics & Applications]*. Springer-Verlag, Berlin.

Cesari, L., 1983. Optimization - Theory and Applications. Problems with Ordinary Differential Equations. Springer-Verlag, Applications of Mathematics, 17.

Cohen, D., Parnas, H., 1976. An optimal policy for the metabolism of storage materials in unicellular algae. Journal of theoretical biology 56, 1–18.

De Mooij, T., Nejad, Z.R., van Buren, L., Wijffels, R.H., Janssen, M., 2017. Effect of photoacclimation on microalgae mass culture productivity. Algal research 22, 56–67.

Faizi, M., Steuer, R., 2019. Optimal proteome allocation strategies for phototrophic growth in a light-limited chemostat. Microbial cell factories 18, 165.

Falkowski, P.G., Raven, J.A., 2007. Aquatic Photosynthesis. Princeton University Press, Princeton.

Foreman-Mackey, D., Hogg, D.W., Lang, D., Goodman, J., 2013. emcee: the mcmc hammer. Publ. Astron. Soc. Pac. 125, 306.

García-Camacho, F., Sánchez-Mirón, A., Molina-Grima, E., Camacho-Rubio, F., Merchuck, J., 2012. A mechanistic model of photosynthesis in microalgae including photoacclimation dynamics. Journal of theoretical biology 304, 1–15.

Geider, R., MacIntyre, H., Kana, T., 1998. A dynamic regulatory model of phytoplanktonic acclimation to light, nutrients, and temperature. Limnology and Oceanography , 679–694.

Geider, R.J., Moore, C.M., Ross, O.N., 2009. The role of cost–benefit analysis in models of phytoplankton growth and acclimation. Plant Ecology & Diversity 2, 165–178.

Giordano, N., Mairet, F., Gouzé, J.L., Geiselmann, J., de Jong, H., 2016. Dynamical allocation of cellular resources as an optimal control problem: Novel insights into microbial growth strategies. PLOS Computational Biology 12, e1004802.

Graff, J.R., Westberry, T.K., Milligan, A.J., Brown, M.B., Olmo, G.D., Reifel, K.M., Behrenfeld, M.J., 2016. Photoacclimation of natural phytoplankton communities. Marine Ecology Progress Series 542, 51–62.

Grima, E.M., Camacho, F.G., Perez, J.S., Sevilla, J.F., Fernández, F.A., Gomez, A.C., 1994. A mathematical model of microalgal growth in light-limited chemostat culture. Journal of Chemical Technology & Biotechnology: International Research in Process, Environmental AND Clean Technology 61, 167–173.

Havelková-Doušová, H., Prášil, O., Behrenfeld, M., 2004. Photoacclimation of *Dunaliella tertiolecta* (chlorophyceae) under fluctuating irradiance. Photosynthetica 42, 273–281.

Hernández Limón, M.D., Hennon, G.M., Harke, M.J., Frischkorn, K.R., Haley, S.T., Dyhrman, S.T., 2020. Transcriptional patterns of emiliania huxleyi in the north pacific subtropical gyre reveal the daily rhythms of its metabolic potential. Environmental Microbiology 22, 381–396.

Jahn, M., Vialas, V., Karlsen, J., Maddalo, G., Edfors, F., Forsström, B., Uhlén, M., Käll, L., Hudson, E.P., 2018. Growth of cyanobacteria is constrained by the abundance of light and carbon assimilation proteins. Cell reports 25, 478–486.

John, D.E., Lopez-Diaz, J.M., Cabrera, A., Santiago, N.A., Corredor, J.E., Bronk, D.A., Paul, J.H., 2012. A day in the life in the dynamic marine environment: how nutrients shape diel patterns of phytoplankton photosynthesis and carbon fixation gene expression in the mississippi and orinoco river plumes. Hydrobiologia 679, 155–173.

MacIntyre, H., Kana, T., Anning, T., Geider, R., 2002. Photoacclimation of photosynthesis irradiance response curves and photosynthetic pigments in microalgae and cyanobacteria. J.Phycol. 38, 17–38.

Mairet, F., Bayen, T., 2020. Parameter estimation for dynamic resource allocation in microorganisms: A bi-level optimization problem, in: Proceedings of the 21st IFAC World Congress.

Mitchell, A., Romano, G.H., Groisman, B., Yona, A., Dekel, E., Kupiec, M., Dahan, O., Pilpel, Y., 2009. Adaptive prediction of environmental changes by microorganisms. Nature 460, 220–224.

Mittag, M., 2001. Circadian rhythms in microalgae, in: International review of cytology. Elsevier. volume 206, pp. 213–247.

Mombaur, K., Truong, A., Laumond, J.P., 2010. From human to humanoid locomotionan inverse optimal control approach. Autonomous robots 28, 369–383.

Moser, H., 1958. The dynamics of bacterial populations maintained in the chemostat. Carnegie Institution of Washington Publication .

Newville, M., Stensitzki, T., Allen, D.B., Ingargiola, A., 2014. LMFIT: Non-Linear Least-Square Minimization and Curve-Fitting for Python. URL: `https://doi.org/10.5281/zenodo.11813`, doi:10.5281/zenodo.11813.

Nikolaou, A., Hartmann, P., Sciandra, A., Chachuat, B., Bernard, O., 2016. Dynamic coupling of photoacclimation and photoinhibition in a model of microalgae growth. Journal of theoretical biology 390, 61–72.

Pavlov, M.Y., Ehrenberg, M., 2013. Optimal control of gene expression for fast proteome adaptation to environmental change. Proceedings of the National Academy of Sciences 110, 20527–20532.

Pontryagin, L., Boltyanskiy, V., Gamkrelidze, R., Mishchenko, E., 1964. Mathematical theory of optimal processes. New York.

Reimers, A.M., Knoop, H., Bockmayr, A., Steuer, R., 2017. Cellular trade-offs and optimal resource allocation during cyanobacterial diurnal growth. PNAS 114, E6457–E6465.

Rudin, W., 1987. Real and complex analysis. Third ed., McGraw-Hill Book Co., New York.

Shuter, B., 1979. A model of physiological adaptation in unicellular algae. Journal of theoretical biology 78, 519–552.

Spolaore, P., Joannis-Cassan, C., Duran, E., Isambert, A., 2006. Commercial applications of microalgae. Journal of bioscience and bioengineering 101, 87–96.

Straka, L., Rittmann, B.E., 2018. Light-dependent kinetic model for microalgae experiencing photoacclimation, photodamage, and photodamage repair. Algal research 31, 232–238.

Sukenik, A., Bennett, J., Mortain-Bertrand, A., Falkowski, P.G., 1990. Adaptation of the photosynthetic apparatus to irradiance in *Dunaliella tertiolecta*: a kinetic study. Plant physiology 92, 891–898.

Sutherland, W.J., 2005. The best solution. Nature 435, 569–569.

Suzuki, L., Johnson, C.H., 2001. Algae know the time of day: circadian and photoperiodic programs. Journal of Phycology 37, 933–942.

Talmy, D., Blackford, J., Hardman-Mountford, N.J., Dumbrell, A.J., Geider, R.J., 2013. An optimality model of photoadaptation in contrasting aquatic light regimes. Limnology and oceanography 58, 1802–1818.

Team Commands, Inria Saclay, 2017. Bocop: an open source toolbox for optimal control. http://bocop.org.

Trélat, E., Zuazua, E., 2015. The turnpike property in finite-dimensional nonlinear optimal control. Journal of Differential Equations 258, 81–114.

Tsiantis, N., Balsa-Canto, E., Banga, J.R., 2018. Optimality and identification of dynamic models in systems biology: an inverse optimal control framework. Bioinformatics 34, 2433–2440.

Waldherr, S., Oyarzún, D.A., Bockmayr, A., 2015. Dynamic optimization of metabolic networks coupled with gene expression. Journal of theoretical biology 365, 469–485.

Wirtz, K.W., Pahlow, M., 2010. Dynamic chlorophyll and nitrogen: carbon regulation in algae optimizes instantaneous growth rate. Marine Ecology Progress Series 402, 81–96.

Zavřel, T., Faizi, M., Loureiro, C., Poschmann, G., Stühler, K., Sinetova, M., Zorina, A., Steuer, R., Červenỳ, J., 2019. Quantitative insights into the cyanobacterial cell economy. eLife 8, e42508.

Zelikin, M.I., Borisov, V.F., 1994. Theory of chattering control. Systems & Control: Foundations & Applications, Birkhäuser Boston, Inc., Boston, MA. URL: http://dx.doi.org/10.1007/978-1-4612-2702-1, doi:10.1007/978-1-4612-2702-1. with applications to astronautics, robotics, economics, and engineering.

Zinser, E.R., Lindell, D., Johnson, Z.I., Futschik, M.E., Steglich, C., Coleman, M.L., Wright, M.A., Rector, T., Steen, R., McNulty, N., et al., 2009. Choreography of the transcriptome, photophysiology, and cell cycle of a minimal photoautotroph, prochlorococcus. PloS one 4, e5135.